Efficacy of a novel sequential enzymatic hydrolysis of lignocellulosic biomass and inhibition characteristics of monosugars

*Sibashish Baksi[1], Akash K Ball[1], Ujjaini Sarkar[*1], Debopam Banerjee[1], Alexander Wentzel[3], Heinz A Preisig[4], Jagdish Chandra Kuniyal[2], Cansu Birgen[4], Sudeshna Saha[1],Bernd Wittgens[3], Sidsel Markussen[3]*

Abstract

Efficient production of sugar monomers from lignocellulose is often hampered by serious bottle-necks in biomass hydrolysis. The present study reveals that ultra-sonication assisted pretreatment following autoclaving, termed as combined pretreatment, can lead to more efficient delignification of lignocellulosic biomass and an open, deformed polysaccharide matrix, found favorable for subsequent enzymatic hydrolysis, is formed. The pattern of inhibition for the enzymatic hydrolysis reaction on combined-pretreated saw dust is identified. Two main inhibition models (competitive and noncompetitive) are proposed and a better fit of experimental values with the theoretical values for the competitive inhibition model validates the proposition that in the present experiment, glucose inhibits the enzymes competitively. Additionally, accuracy of the inhibitory kinetics based models is estimated over a series of enzyme and substrate concentrations. A prominent departure in the range of residual concentrations from the competitive model supports the same proposition, in comparison to the non-competitive model.

Key words: enzymatic hydrolysis; enzyme inhibition; lignocellulose, cellulase; xylanase; β-glucosidase.

1.

1. Introduction

With increasing global population and industrialization, the energy demand and consumption rates have been increasing progressively for the last few decades. Although fossil fuels are still the most convenient and promising source to meet this elevated energy demands, its sources are slowly depleting. Moreover, its exploitation is directly linked to global warming, environmental pollution, climate change and health hazards(Lavoine, Desloges, Dufresne, & Bras, 2012). Thus, there is an urgent need to find alternative energy resources. Along with nuclear-, solar-, wind-and hydro-power, biofuel represents an important future energy carrier and a sustainable substitute for fossil fuels. In this context, the biofuel production from Lignocellulosic Biomass (LB) is gaining importance due to its abundance and sustainable production process. Lignocellulosic biomass, essentially consisting of cellulose, hemicelluloses and lignin are considered as the primary feedstock for production of biofuels.

Lignin forms a hetero-matrix with sugar polymers by cross-linking via hydrogen bonding, covalent bonding such as ester linkages and physical encrustation. In the hetero-matrix, cellulose molecules form the inner core of the structure, which is surrounded by a lignin-hemicellulose based cross-linked matrix. It is essential to remove lignin from lignocellulose feedstock in order to efficiently access the reducible sugar polymers for hydrolysis using enzymes (Agbor, Cicek, Sparling, Berlin, & Levin, 2011; Betts, Dart, Ball, & Pedlar, 1991; Hu & Ragauskas, 2012).

Over the years, many approaches are developed and implemented to generate biofuels from LB. Some of the most popular methods adopted for initial pretreatment of biomass include conventional alkaline peroxide-based pretreatment, acid pretreatment, steam explosion, ammonia fiber expansion (AFEX), hot liquid water pretreatment, etc. While several processes remove lignin efficiently from LB, it is found that a large portion of hemicelluloses and celluloses degrade due to the high temperature often applied (Y. Sun & Cheng, 2002).

Consequently, a number of soluble toxic chemicals like furfural and HMF are generated along with the degradation of hemicelluloses (W.-H. Chen, Hsu, Lu, Lee, & Lin, 2011). AFEX pretreatment generates much smaller amount of inhibitors and increases the surface area considerably, but it is not effective in removing lignin from biomass with high lignin content. In spite of being very efficient, acid pretreatment is environmentally incompatible since significant amounts of toxic chemicals and inhibitors are formed. Additionally, corrosion is also a major concern of acid pretreatment (Wu, Yu, Chan, Kim, & Mai, 2000; Yoon, Wu, & Lee, 1995; Zhu, Pan, & Zalesny, 2010). Considering the advantages, disadvantages and cost of all pretreatment procedures, conventional alkaline peroxide pretreatment is found to be a promising cost-effective option for pretreatment with much less production of inhibitors.

Enzymatic hydrolysis of delignified biomass liberates fermentable sugars from pretreated LB, with commercial enzymes, for decades. However, improved hydrolysis protocols are still needed in order to overcome various problems arising due to the presence of inhibitors during hydrolysis. Typically, two types of inhibition are observed during enzymatic hydrolysis of LB - *product inhibition* and *substrate inhibition*. A couple of research groups tried to overcome inhibition by using enzymes extracted from different genetically modified organisms, significant progress is yet to be made (Fenila & Shastri, 2016; Sternberg, Vuayakumar, & Reese, 1977).

Morus serrata (MS, mulberry), popularly known as Himalayan Mulberry, is a promising LB source as this species can be used to generate monomeric sugars. Its optimum temperature for growth ranges from 18°Cto 30°C(Arya, Kalia, & Arya, 2000; Sargent, 1896).MS is widely used in wood technology-based industries. A huge amount of wood powder is generated from MS, which is generally discarded as waste. However, this powder can be used as a prospective source of LB for generation of monomeric sugars. Other than lignin and

carbohydrate, various components present in other different types of biomass accounting for the undetermined portion are enlisted below (Table 1).

Table 1 Components present in various other types of biomass accounting for the undetermined portion (*other than lignin and carbohydrate*).

Biomass	Components	References
Switch grass	proteins, waxes, resins, gums, chlorophyll	(Xu, Cheng, Sharma-Shivappa, & Burns, 2010)
Bermuda Grass	uronic acids, acetyl groups, minerals, waxes, resins, gums	(Wang, Keshwani, Redding, & Cheng, 2010)
Hybrid popler	ash, acetyl, anhydroglucuronic acid	(Luo, Brink, & Blanch, 2002)

In the present study, LB from MS is first de-lignified using a novel two-step pretreatment process and subsequently de-lignified biomass is hydrolyzed using a specific enzyme protocol to maximize both C_6 and C_5 sugars. Two inhibition models, competitive and non-competitive, are validated for various ranges of substrate and enzyme concentrations in order to generate primarily glucose and xylose.

2. Materials and Methods

2.1. Sample preparation

After harvesting branches from MS trees by using a hand saw, Himalayan Mulberry chips and sawdust are prepared by using a chain saw (Make: STIHL, Germany; Model: Cast Iron Chain Saw; Material: MS-180) and a circular saw (Make: BOSCH; Model: GKS190). Finely

ground mulberry powder is then passed through a 85 mesh screen size sieve prior to be further used in order to remove impurities and larger particles.

2.2. Pretreatment

A range of different combination of pretreatment protocol is applied to maximize the removal of lignin from mulberry samples while minimizing biomass denaturation and formation of inhibitors for subsequent hydrolysis.

2.2.1. Alkaline peroxide pretreatment

Conventional alkaline-peroxide pretreatment (AP) is performed using 25 g moisture free mulberry powder with a solid to alkaline-peroxide solution ratio of 1:40 (w/v) for 5h at 50°C. The alkaline peroxide solution consists of 2% H_2O_2 [v/v] where the pH is maintained at 11.5 with NaOH. Alkaline peroxide pretreatment is performed with agitation at 150rpm (Banerjee, Car, Scott-Craig, Hodge, & Walton, 2011).

2.2.2. Combined pretreatment

A novel combined pretreatment (CP) procedure is introduced to maximize removal of lignin from the wood sample. 25 g of moisture free wood sample is submerged in alkaline solution (pH 11.5), prepared by dissolving NaOH pellets into distilled water, followed by autoclaving at 121°C for 60 min. Successively, the solid fraction is isolated, washed and dried at 40°C. Next, the dried sample is submerged in 2%alkaline-peroxide solution [v/v] (pH 11.5) and sonicated 20 times using a probe sonicator [Make: PCI analytics, India; power used: 300W; probe diameter: 9mm]. After sonication, the solid fraction is separated by filtration using Whatman no. 1 filter papers (Make: Sartorius, Germany), neutralized with de-ionized water and dried overnight in a hot air oven at 40°C. The dried, sonicated mulberry powder is then again treated with alkaline peroxide solution [pH 11.5, 2% H_2O_2(v/v)] for 5h at 50°C. Subsequently, the insoluble solid material is separated and washed with de-ionized water

112 until pH of the solution is at neutral. Finally, the sample is again dried overnight in a hot air
113 oven at 40°C.

114 *2.3. Isolation of hemicellulose from pretreatment solutions*

115 Hemicelluloses have a tendency to dissolve in acid or concentrated alkaline solution and can
116 be isolated by precipitation. After pretreatments followed by separation (*see* section 2.2), the
117 alkaline peroxide solution is acidified to a pH of 4.4 using 10%HCl [v/v] solution. Next, three
118 volumes of 95% ethanol is added to the acidified solution and incubated overnight, allowing
119 the dissolved hemicelluloses to precipitate. Hemicelluloses thus precipitated are recovered
120 afterwards by filtration and then washed with 72% ethanol followed by drying(Subhedar &
121 Gogate, 2014).

122 *2.4. Estimation of lignin content in the biomass*

123 The amount of lignin present in untreated as well as in the pretreated mulberry wood powder
124 is determined quantitatively following TAPPI T222 method (Tappi, 2002). Specifically, 1g
125 (±0.1 g) of each sample (test specimen) is dissolved in 15ml of 72% sulfuric acid and
126 incubated at 20°C for 2h.Then,the final volume is adjusted to 575ml with distilled water and
127 the mixture is boiled for 4h and left overnight for precipitation of lignin. The precipitated
128 lignin is isolated using a glass crucible and quantified along with acid-soluble lignin
129 (Standard, 2002).

130 $$Lignin(\%) = \frac{Weight\ of\ lignin\ (g)}{Weight\ of\ the\ test\ specimen(g)} \times 100 \qquad (1)$$

131 Where weight of the lignin (g) = [weight of the crucible with lignin (g) -weight of the
132 crucible (g)].

133 *2.5. Estimation of total carbohydrates in crude and pretreated mulberry wood powder*

134 Total reducing sugar in crude and pretreated sample are determined with 3,5-dinitrosalicylic
135 acid (DNS method) using glucose as the standard(Miller, 1959; Sluiter et al., 2008; Y. Sun &
136 Cheng, 2005; Van Wychen & Laurens, 2017). 0.3 g each of the samples is hydrolyzed with
137 3ml of 72% H_2SO_4 and the mixture is kept at 30°C for 1h. Afterwards, the solution is diluted
138 to 4% $H_2SO_4$by adding 84 ml of distilled water followed by autoclaving for 1h. Next the
139 mixture is centrifuged and the clear supernatant is collected. 3 ml of clear supernatant is
140 mixed with 3 ml of DNS reagent and boiled for 5 min at 100°C.Then the mixture is cooled
141 down and the color intensities are recorded in a UV/Vis spectrophotometer [Make:
142 PerkinElmer, USA; Model: Lambda 365] at 575nm. Quantitative estimation of total reducing
143 sugar is based on the standard curve generated using glucose equivalent.

144

145 *2.6. Crystallinity of biomass using X-Ray Diffraction (XRD) method*

146 Changes in the crystallinity of biomass depend largely on the specific method of
147 delignification as crystalline and amorphous cellulose along with lignin and hemicelluloses
148 largely constitute the structure of the biomass matrix. The degree of crystallinity of crude and
149 pretreated biomass is determined using an X-ray diffractometer [Make: Rigaku, Japan;
150 Model: Giegerflex D/Max B], employing a Cu kα radiation source functioning at 40kV and
151 30 mA. Scan is performed in the range of 2θ [Bragg angle=5°- 40°] at a scanning rate of
152 0.05° per second. The crystallinity index (CrI) of various samples is determined using the
153 scattered data in equation (2)(Baksi et al., 2018; Zhang et al., 2014):

154 $$CrI\ (\%) = \frac{I_{002} - I_{am}}{I_{002}} \times 100 \qquad (2)$$

I_{002} and I_{am} represent the scattered intensity of the crystalline portion of biomass at about 2θ= 22.5°and the amorphous portion of biomass at about 2θ= 16.8°, respectively.

2.7. Enzymatic hydrolysis

Enzymatic hydrolysis is carried out using a cellulase blend (SAE0020, 1000U/g, 1.2g/ml) along with cellulase [C1184, 1.3U/mg, derived from *A. niger*], hemicellulase [H2125,1.5U/mg, derived from *A. niger*] and β-glucosidase [49290, 7.7 U/mg, derived from almonds].Using these enzymes, a cocktail is prepared with a ratio of cellulase mix: hemicellulase :β-glucosidase= 1:1:2 [unit basis], whereas the cellulase mix is prepared using cellulase blend [SAE0020] and cellulase [C1184] with a ratio of 1:1.8 [unit basis].

Enzymatic hydrolysis is performed in a stoppered conical flask in 50 ml solution of citrate buffer (pH 4.8) along with sodium azide [0.1% (w/v)] in order to inhibit microbial contamination. A series of hydrolysis experiments is performed, using different enzyme cocktail (mix) concentrations (1.28, 6.66, 11.23 and 17.8g/L) at three different substrate[pretreated mulberry powder] loadings(25, 50and125 g dry biomass/L). In each hydrolysis experiment, every substrate (25, 50and 125 g dry biomass/L) is supplemented with 0.2 g of hemicelluloses, taken from pretreatment liquor precipitate. Initially, the reaction mixture, comprising of substrate, buffer and sodium azide, is agitated at 115 rpm. When the temperature reached 50° C, enzymes are added into the reaction mixture to initiate hydrolysis. Samples are withdrawn from the reaction mixture at different time intervals and placed in a boiling water bath for 10 minutes to terminate the reaction by deactivating the enzymes. Thereafter, free sugars are estimated using High Performance Liquid Chromatography (HPLC).

2.8. Analysis of sugars by HPLC

Quantification of hydrolyzed sugars is carried out using HPLC (Make: Waters; Model: 2489) fitted with an RI detector (Make: Waters; Model: 2414) for measuring the change in refractive index of the column effluent passing through the flow-cell. A Brownlee amino column (Make: PerkinElmer, USA; Material: N9303501) is used to separate sugars at ambient temperature. The mobile phase used consists of HPLC grade acetonitrile and ultrapure water [70:30 (v/v)] at a constant flow rate of 0.6 ml/min. The temperature of the RI detector is maintained at 45°C with a sensitivity of 16, while the column temperature is kept at 30°C.Sugars are finally quantified using standard curves generated with standard grade glucose (CAS No.: 50-99-7) and xylose (CAS No.: 58-86-6).

2.9. Proposed enzyme kinetics

Enzymatic hydrolysis is a complicated process as it comprises of heterogeneous substrate and an enzyme blend composed of endoglucanase (EG), cellobiohydrolase (CBH), β-glucosidase (BG) and hemicellulase (XY). The overall phenomena of hydrolysis of biomass can be described with the help of two heterogeneous reactions as follows:

$$Cellulose(S) \xrightarrow[CBH]{EG} Cellobiose(O) \overset{BG}{\Leftrightarrow} Glucose(G)$$

$$Hemicellulose(S) \xrightarrow{xylanase} Xylose(X)$$

The activity of an enzyme is directly correlated with its initial hydrolysis rate as well as the maximum velocity of hydrolysis.

It is well established that the enzyme activity is inhibited with an increase in product (*cellobiose* and *glucose*) concentration during enzymatic hydrolysis(Bezerra, Dias, Fraga, & Pereira, 2006). Two types of inhibition, namely, competitive and noncompetitive, are

predominately present in hydrolysis systems and responsible for inhibiting enzyme activity. In order to assess the type of inhibition present, time-integrated expressions of competitive and noncompetitive models are considered(Andrić, Meyer, Jensen, & Dam-Johansen, 2010), *see* Table 2:

Table 2 Equations of competitive and noncompetitive inhibition.

Inhibition model	Equations	
Competitive	$t = \frac{1}{k_{cat}E_0}\left(-\left(K_M + \frac{K_M}{K_I c}(cG_0 + S_0)\right)\ln\left(1 - \frac{c(G - G_0)}{S_0}\right) + \left(1 - \frac{K_M}{K_I c}\right)c(G - G_0)\right)$	(3)
Non-competitive	$t = \frac{1}{k_{cat}E_0}\left(-\left(K_M + \frac{K_M}{K_I c}(cG_0 + S_0)\right)\ln\left(1 - \frac{c(G - G_0)}{S_0}\right) + \left(1 - \frac{K_M}{K_I c}\right)c(G - G_0) + \frac{c}{2K_I}(G^2 - {G_0}^2)\right)$	(4)

Here, k_{cat} is the apparent cellulase turn-over number, E_0 is the initial enzyme concentration (g/L), K_I is the enzyme–glucose complex dissociation constant or inhibition constant, whereas K_M represents the apparent Michaelis constant, which corresponds to the affinity between cellulose and cellulase. S_0 and G_0 stand for initial concentration of cellulose from pre-treated saw dust (g/L) and initial glucose concentration (g/L), respectively. *c* (=0.9) represents the reciprocal value of the number of glucose units present in a molecule of cellulose obtained from pre-treated saw dust. In order to evaluate the proposed models with experimental data, it is necessary to find out the values of the apparent cellulase turn-over

number k_{cat} and the inhibition constant K_I for each of the substrate loadings (25, 50, and 125g/L), hydrolyzed with predetermined enzyme concentrations (1.28, 6.66, 11.23, 17.8g/L). The apparent kinetic parameters of the inhibition models are evaluated using a nonlinear least-square method. Each model is regressed on all available data. The quality assessment of the model prediction of net glucose concentration is based on the R^2 value of each of the nonlinear fits. The solution algorithm is developed with the help of MATLAB R2017a using the ode45[1] function. Based on a suitable fit of the kinetic model with the experimental data, the mode of inhibition executed by the end product (glucose) is estimated.

3. Results and Discussion

3.1. Chemical composition of saw dust

The chemical composition of crude Himalayan mulberry wood dust and its modifications during various stages of pretreatment is estimated (refer Table 3).

Table 3 Modification of chemical composition at different stages of combined pretreatment (CP) of Himalayan mulberry wood powder.

Various Stages of Pretreatment	Composition (Dry wt %)					
	Lignin	Glucan	Xylan	Mannan	Galactan	Other (Ash, Wax, Extractives) (wt %)
Crude	32.1±0.03	44.8±0.4	6.24±0.2	8.5±0.06	4.3±0.2	4.06±0.1

[1]*ode45 is a very useful function for solving non-stiff ordinary differential equation and it is a medium order method.*

Autoclave (at 121°C for 1h)	29.77±0.3	52.27±0.2	17.96±0.4	-	-	-
Probe sonication (for 1h)	25.83±0.2	56.44±0.2	17.73±0.3	-	-	-
Alkaline-peroxide pretreatment (5h at 50°C)	23.97±0.3	58.38±0.89	17.65±0.2	-	-	-

It is observed from the table that crude Himalayan mulberry wood powder contains 44.8% glucan whereas three different hemicellulosic sugars like xylan (6.24%), Mannan (8.5%) and Galactan (4.3%) are also found in mulberry wood powder. Glucanis found as the corner-stone of the lignocellulosic biomass and hemicellulosic sugars like mannan and xylan often exist in a complex with Glucan and galactan, termed as glucomannan, (galacto) glucomannan and glucoxylan(Geng, Sun, Sun, & Lu, 2003). Following Combined Pretreatment (CP), a considerable depletion of lignin is observed along with elevation of glucan and xylose content (Table 3) in relative percentages. However, no traces of mannan and galactan are found in the biomass following combined pretreatment. Alkaline-peroxide pretreatment is strongly correlated to primary solubilization and partial degradation of the macromolecular hemicelluloses (J. Sun, Mao, Sun, & Sun, 2005).This significant increase in the xylose content, following combined pretreatment, provides an evidence that in the mulberry wood cell walls, xylose resides in the main chain of hemicelluloses while galactose and mannose are probably present in side chains and are thus released relatively easily after pretreatment of

moderate severity. Dissolution of all galactose from Douglas fir (*Pseudotsuga menziesii*) wood chips after only 30 min of pretreatment with 2% alkaline-peroxide pretreatment is also reported (Alvarez-Vasco & Zhang, 2013). Removal of galactose strongly assists in solubilizing the glucomannan structure. Even at low temperature (93°C), as soon as the wood powder comes in contact with alkaline-peroxide solution, significant loss of glucomannan (=75%) is reported (Wigell, Brelid, & Theliander, 2007). Moreover, presence of hydrogen peroxide also facilitates removal of mannan moieties significantly from biomass (Alvarez-Vasco & Zhang, 2013).On the other hand, xylan has a removal pattern that differs significantly from that of glucomannan. A combination of high temperature and higher peroxide concentration is needed to dissolve and remove xylose moieties present in the major backbone chain of hemicelluloses. A limited loss of xylose is reported at temperatures below 139°C (Fang, Sun, & Tomkinson, 2000; Wigell et al., 2007).

3.2. Effect of various pretreatment procedures on mulberry powder

Starting with an untreated biomass with a lignin content of 32.1 % (dry weight), CP is found to remove lignin from untreated biomass more efficiently (23.97 %of dry weight remaining) than alkaline peroxide (AP) based pretreatment (28.61% of dry weight remaining).Amount of total carbohydrates increases from 63.84 wt % to 68.75 wt % following AP whereas to 74.03 wt % after CP. From this scenario, it can be inferred that combined pretreatment is substantially more efficient as compared to AP for optimum delignification. This is crucially beneficial for downstream enzymatic hydrolysis of the pretreated biomass.

There are various types of covalent and non-covalent linkages present in the lignocellulosic matrix that make the matrix stable. Two important chemicals used in AP are NaOH and H_2O_2. In alkaline conditions, H_2O_2 is readily decomposed into hydroxyl radicals and superoxide anions. These radicals cleave several inter-unit bonds, introducing hydrophilic

carboxyl groups into the lignin structure and eventually dissolve lignin and hemicelluloses into the pretreatment solution(Betts et al., 1991). While several ester and ether bonds are easily broken during alkaline pre-treatment, most of these covalent bonds remain intact. In CP, the mulberry powder is treated in an autoclave [pressure=15psi (*gauge*)], where high pressure and temperature substantially help deforming the LB heteromatrix.Subsequently, ultrasonic waves generate bubbles, which on collapsing due to wave compression, form micro-jets enabling the cell walls to break, thereby deforming the matrix to a great extent with an effective increase in the available surface area. This likely allows the radicals formed from H_2O_2 to access a larger surface area of the lignocellulosic matrix at a time. Eventually these radicals break and saponify more bonds present in the matrix. The dark brown color of untreated biomass is transformed to light yellow after delignification followed by washing [see Figure 1].

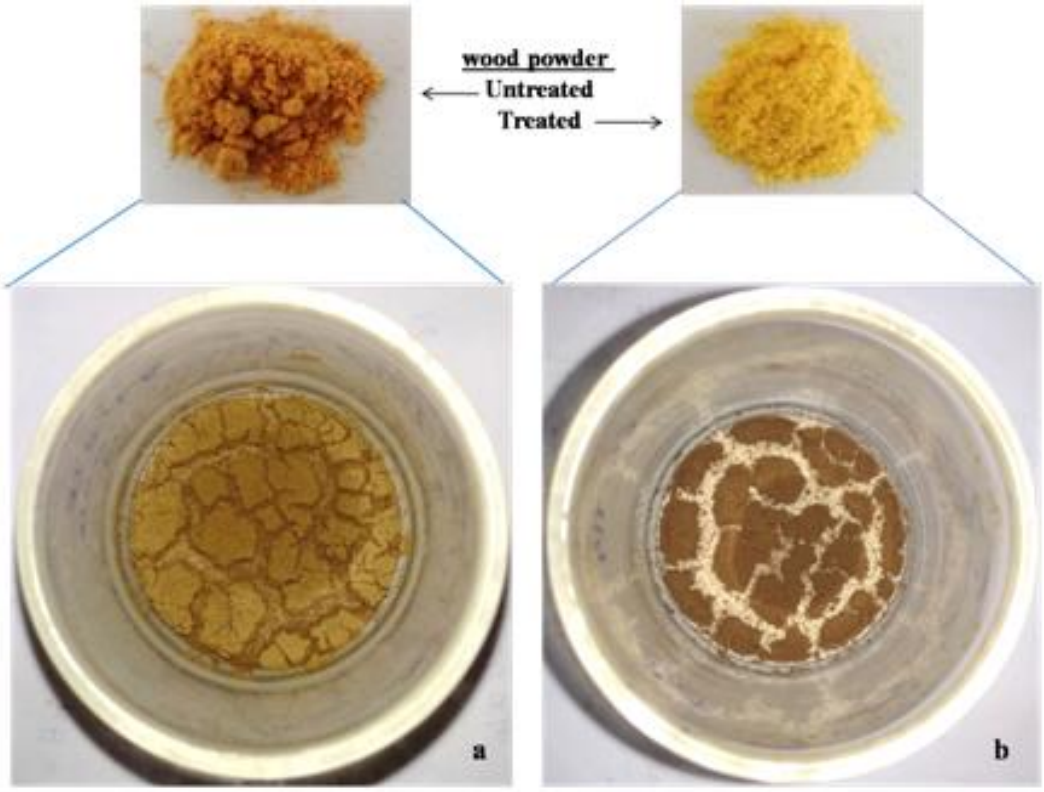

Figure 1 Acid insoluble lignin, on crucible bed, obtained from (a) untreated material and (b) pretreated material (CP).

Obviously, removal of lignin (brown colour) from the wood powder causes discoloration of the material. Additionally, being an efficient procedure for optimum delignification of mulberry wood powder, pretreatment liquors acquired during various steps of combined pretreatment (step I: autoclave, step II: probe sonication and step III: 5h long pretreatment with alkaline-peroxide solution) are collected and then dissolved fractions of hemicelluloses are precipitated from the liquor. A cumulative amount of 10.5% of total hemicelluloses is finally recovered following CP and the same is further hydrolyzed along with pretreated biomass (CP), in the downstream enzymatic hydrolysis.

3.3. Crystalline structure of biomass

The crystalline fingerprints of untreated and combined pretreated mulberry powder are determined using XRD analysis as represented in Figure 2.

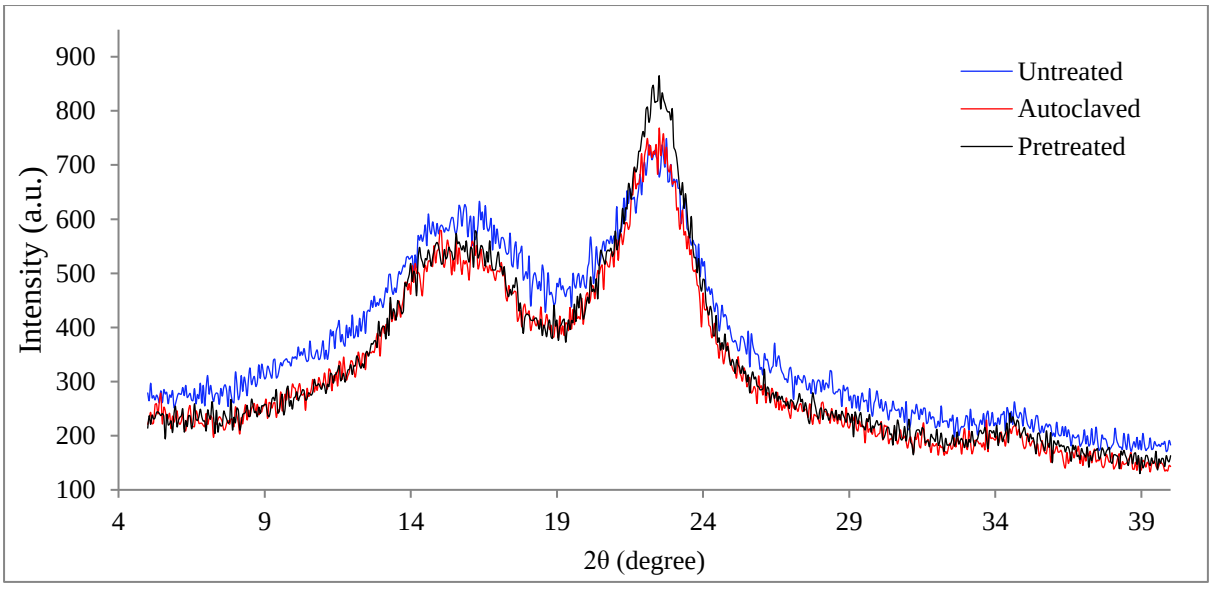

Figure 2 X-Ray diffraction patterns of untreated, autoclaved and pretreated (CP) material.

The XRD diffraction pattern of each sample exhibited two sharp peaks at around 2θ=22.5° and 16.8° which correspond to the (2,0) and (1,0) lattice planes of crystalline cellulose I, respectively(S. Chen, Ling, Zhang, Kim, & Xu, 2018). Crystallinity of the mulberry powder significantly increase after combined pretreatment (see Figure 2).Crystallinity of the untreated materials is calculated as 19.91% whereas after autoclaving, the crystallinity increases to 33.98% and eventually to 41.39% after completion of combined pretreatment. This finding indicates removal of amorphous portion from the solid biomass material with subsequent liberation of crystalline cellulose. Due to the exposure of untreated material to high temperature and pressure during autoclaving, most of the bonds present in the amorphous region of the lignocellulosic matrix might have broken. Further exposure of the autoclaved material to ultra-sonication and downstream 5h long alkaline-peroxide treatment might have helped in breaking the additional covalent and non-covalent bonds in the amorphous region. Amorphous regions of lignocelluloses are composed of lignin and hemicelluloses. It is therefore evident that combined pretreatment leads to cleavage of bonds in this region and eventually solubilize hemicelluloses and lignin in the pretreatment liquor and finally increases the global crystallinity of biomass.

3.4. Enzymatic saccharification of combined pretreated (CP) mulberry powder

The results of enzymatic hydrolysis of pretreated mulberry sawdust are shown in Fig.3. It is evident from Fig.3 that, for a particular substrate concentration, yield of total reducing sugar increases with an escalated enzyme concentration, varying in the range of 1.28 g/L to 17.8 g/L. Additionally, the effect of substrate loading for a particular enzyme concentration can also be explained from the figure. An increased amount of total reducing sugar can be achieved with a particular enzyme concentration by increasing substrate loading from 25g/L

to 50 g/L. Surprisingly, further increment of substrate loading till 125 g/L resulted in a sugar yield lower than the same achieved with 50 g/L substrate concentration. The concentrated (125 g/L substrate) reaction mixture forms a thick slurry that induces mass transfer limitation, thereby apparently reducing the sugar yield (O'Dwyer, Zhu, Granda, & Holtzapple, 2007).

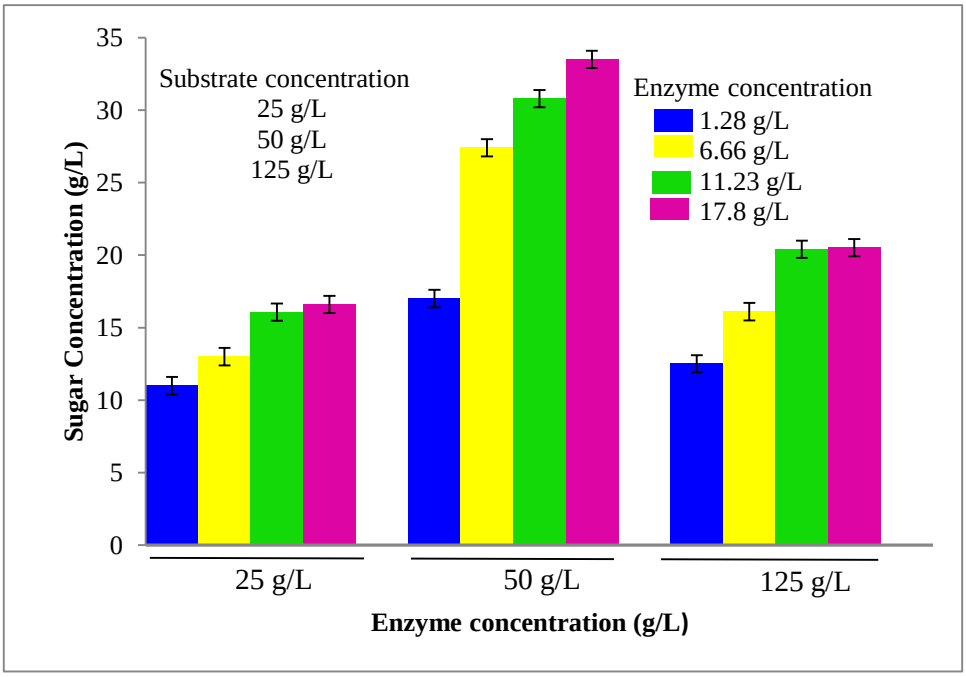

Figure 3 Yield of total reducing sugar (g/L) using various substrate (25, 50, 125 g/L) and enzyme (1.28, 6.66, 11.23, 17.8 g/L) concentrations.

Apart from glucose, xylose is considered as the second most important monomeric sugar for downstream fermentation to generate second generation biofuel. Therefore, in the present study, individual C5 (xylose) and C6 (glucose) sugar concentrations generated under each hydrolysis condition are measured for about 3 days and analyzed using HPLC. Results are shown in Fig.4. During initial stages of hydrolysis, xylose liberates at a higher rate than glucose. At around 10 h of hydrolysis, xylose reaches an equilibrium concentration. Xylanase, present in the enzyme system obviously attacks the hemicellulose fraction of the

biomass efficiently and hydrolyzes it rapidly during the initial stages of hydrolysis, before getting deactivated due to product (glucose) inhibition.

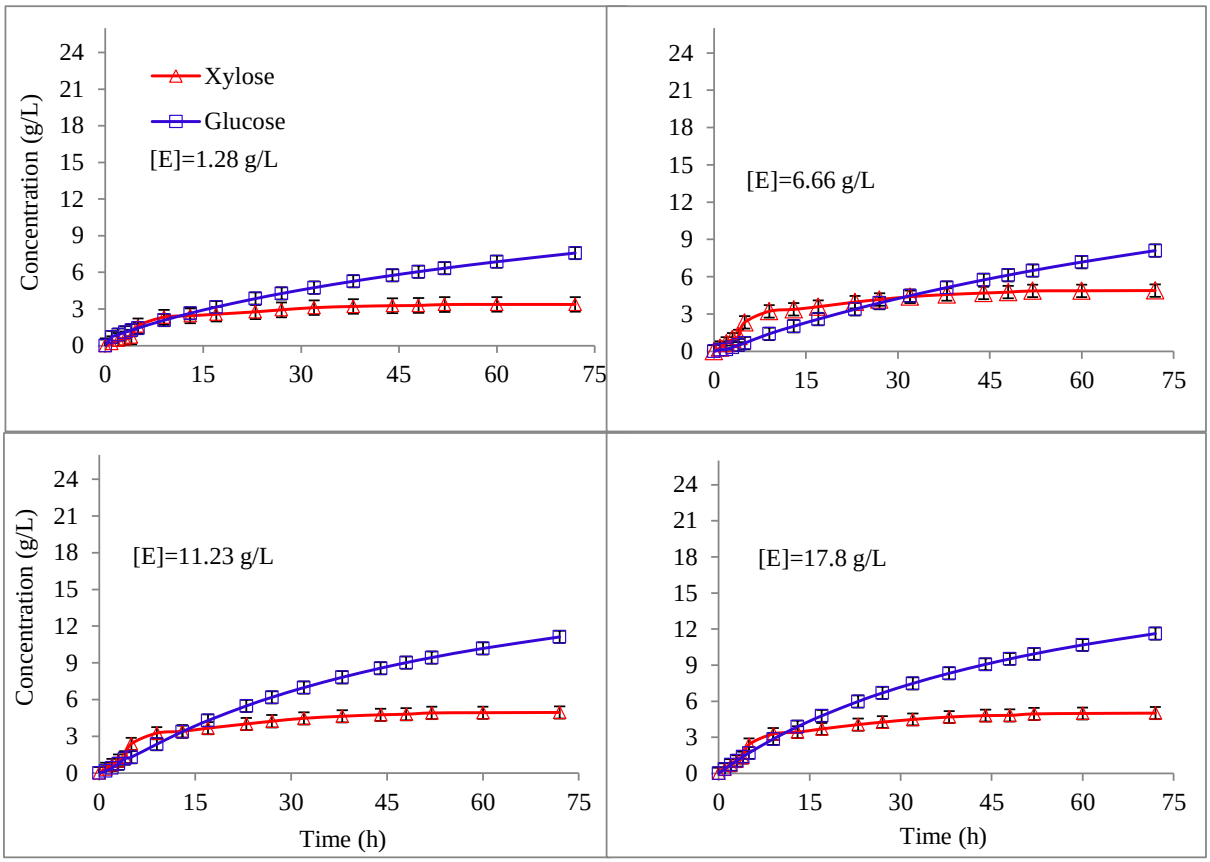

Figure 4(a)

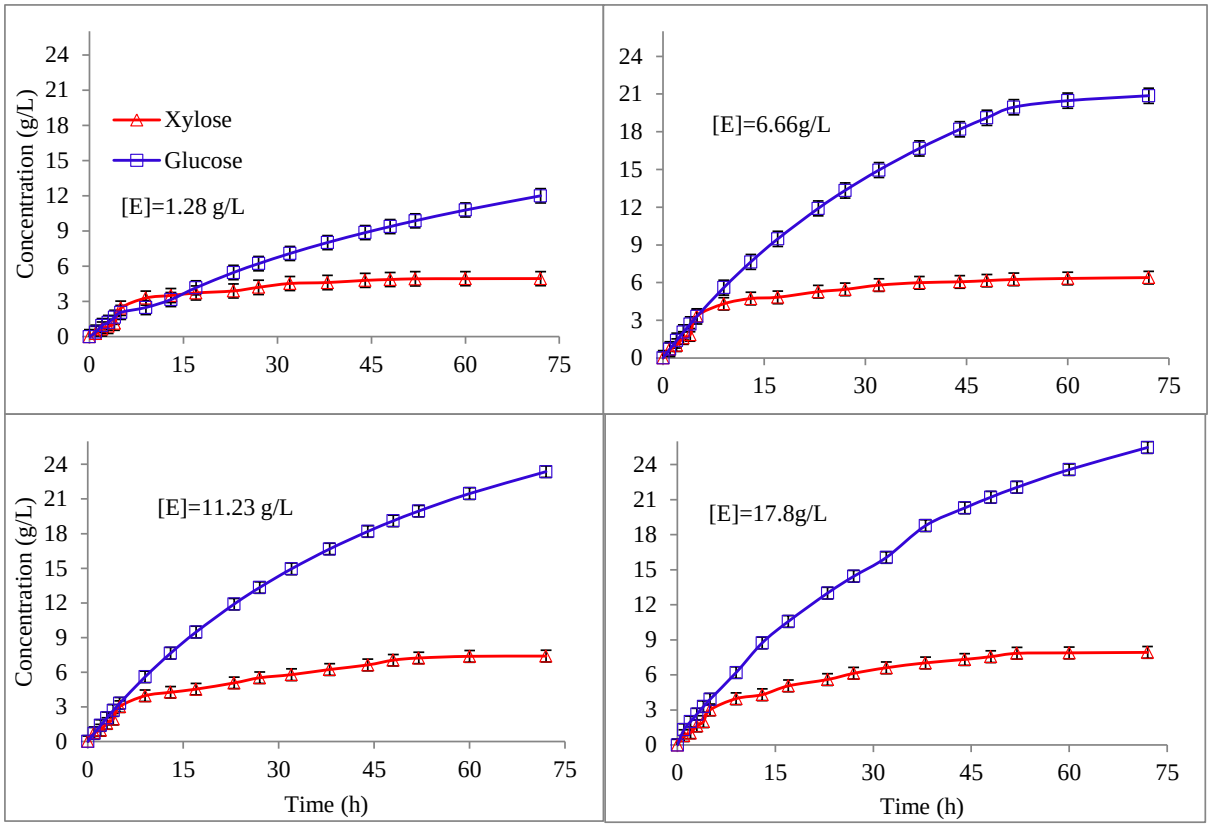

347

348 Figure 4(b)

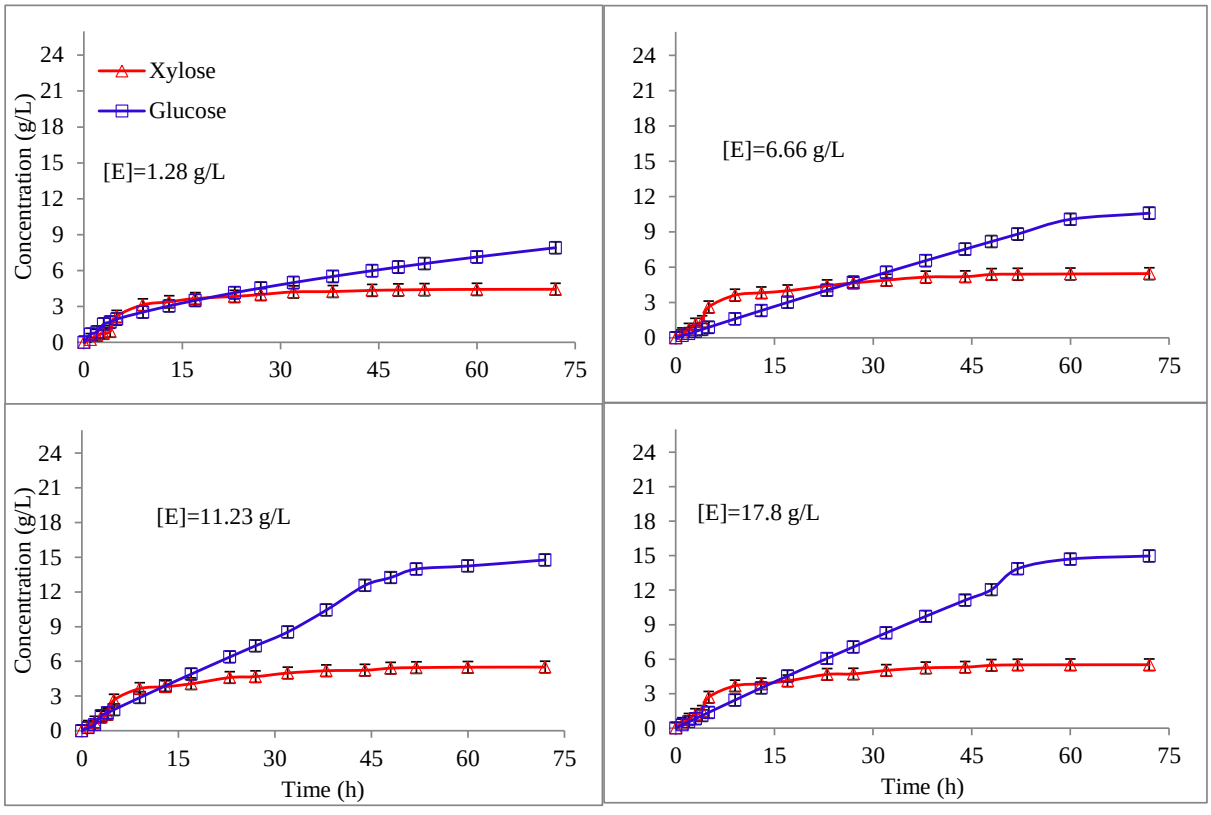

349

350 Figure 4(c)

Figure 4 Time dependent production of glucose and xylose from pretreated biomass with different enzyme concentrations (a) 25g/L (b) 50g/L, (c) 125g/L.

Most likely product inhibition is not solely responsible for the rapid fall in xylose generation rate. In fact, inhibitory effects exhibited by hemicellulose derived sugars are known to be much less significant than the same by glucose (Xiao, Zhang, Gregg, & Saddler, 2004). It is inferred that before 10 h of hydrolysis, all immediately accessible hemicellulose get hydrolyzed. Also, any further increase in xylose concentration (at a much lower rate) is connected to the hydrolysis of cellulose, proceeding, successively giving access to further xylose moieties for hydrolysis (Lin, Yan, Liu, & Jiang, 2010).

At the same time, hydrolysis of cellulose to glucose proceeds at a lower rate than xylose liberation but proceeds for much longer time and at a successively decreasing rate. Exo- and endo-glucanase both attack and hydrolyze cellulose chains from cellulose fibrils attached to the core matrix, followed by generation of cellobiose, while β-glucosidase immediately starts hydrolyzing cellobiose molecules into glucose. Successive decrease in glucose production rate is probably due to successive increase in feedback inhibition by the accumulating glucose (Lai et al., 2014; Li et al., 2013). Total glucan and xylan recovery are estimated after hydrolysis is complete (see Table 4).

Table 4 Carbohydrate recovery following completion of hydrolysis after combined pretreatment (CP).

Substrate	Enzyme	Carbohydrate conversion and yield

concentration (g/L)	Concentration (g/L)	Glucan conversion (%)	Glucose Yield (%)	Xylan conversion (%)	Xylose Yield(%)
25	1.28	51.07	45.963	39.95	35.156
	6.66	54.58	49.122	58.03	51.0664
	11.23	74.93	67.437	58.86	51.7968
	17.8	78.30	70.47	59.45	52.316
50	1.28	38.36	34.524	40.15	35.332
	6.66	71.50	64.35	51.91	45.6808
	11.23	80.06	72.054	60.01	52.8088
	17.8	87.26	78.534	64.23	56.5224
125	1.28	10.83	9.747	17.03	14.9864
	6.66	14.49	13.041	20.95	18.436
	11.23	20.23	18.207	21.14	18.6032
	17.8	20.50	18.45	21.18	18.6384

373

374 It can be seen from Table 4 that with a particular substrate-enzyme combination, a relatively
375 greater percentage of glucan is recovered with a relatively less amount of xylose. Similar
376 kind of outcome is reported where 85% glucan and 70% of xylose have been achieved with

377 an enzyme cocktail composed of cellulase, beta-glucosidase, xylanase and β-xylosidase (Qing
378 & Wyman, 2011). On the other hand, a similar trend is observed with a recovery of 40%
379 glucan and 27% xylan using an enzyme-cocktail, composed of endoglucanase,
380 cellobiohydrolase, β-glucosidase, endoxylanase, β-xylosidase and acetylxylan esterase (Barr,
381 Mertens, & Schall, 2012). These results elucidate that efficient and complete hydrolysis of
382 xylan is partially hindered due to the structural complexity of hemicellulose along with
383 specific requirements of hemi-cellulolytic enzymes (like formation of a precise transition
384 state in order to bind the substrate more efficiently and effectively). Additionally, the
385 competition between cellulase and hemicellulase for binding on the reactive sites of cellulose
386 make hemicellulase limited for xylan hydrolysis. Stronger binding of cellulase to xylan in
387 comparison to glucan, makes xylan occupied with cellulase faster. As a result, xylanase,
388 present in hemicellulase, cannot bind efficiently with xylan backbone and the same is another
389 potential reason for the incomplete hydrolysis of xylose. Chemical structure and
390 modifications also play a crucial role in the hydrolysis of xylan. Presence of substitutes like
391 4-O-Meglucuroic acid in xylan backbone can potentially deactivate endoxylanase (Barr et al.,
392 2012). Acetylation of xylan can also inhibit endoxylanase to a great extent. As these
393 substitutes are removed, during pretreatment and enzymatic hydrolysis, xylan becomes less
394 soluble and form aggregates that offers steric-hindrance, thereby retarding de-polymerization
395 (Wyman et al., 2005).

396

397 *3.5. Determination of Inhibition pattern and kinetic parameters*

398 In enzyme-substrate systems, two types of inhibition can be present: substrate inhibition and
399 product inhibition. Product inhibition has a serious influence on cellulose hydrolysis and
400 enzyme kinetics (Corazza, Calsavara, Moraes, Zanin, & Neitzel, 2005). Based on this and the
401 observation of successive decrease in glucose production rate in Fig.4., inhibition kinetics

associated with glucose production is investigated. A schematic diagram of inhibition phenomena is presented in Fig.5. (Andrić et al., 2010).

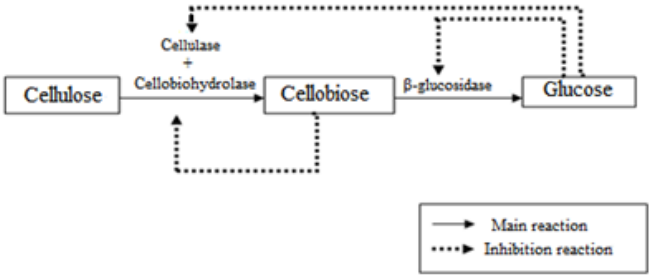

Figure 5 Schematic representation of probable inhibition phenomena during enzymatic hydrolysis of LB.

Though cellobiose and glucose both act as inhibitors during enzymatic hydrolysis of lignocellulosic biomass, specific inhibition type(s), exerted only by glucose is considered here. However, the biomass is a heterogeneous substrate and the commercial cellulolytic enzyme system can be composed of different numbers and types of enzymes. It is reasonably difficult to measure the initial intrinsic or apparent hydrolysis rate for this cellulose-cellulase system. Thus, Dixon or Lineweaver-Burk plots cannot be applied for evaluating the type of inhibition exhibited by glucose (Zhao, Wu, Yan, & Gao, 2004). Competitive inhibition occurs in cellulose-cellulase systems and in between glucose and β-glucosidase (Andrić et al., 2010; Lee & Fan, 1983). In competitive inhibition, the product competes with the substrate for binding to the active site of the enzyme and inhibits it. Increasing the substrate concentration is a way to overcome competitive inhibition exerted by the key product. In the present study, increased product recovery is observed by increasing the substrate concentration from 25 g/L to 50 g/L (*see* Fig. 3.). Following hydrolysis of 25g/L concentrated substrate with predefined enzyme concentration, glucose

and xylose are produced as products and both compete for the active sites of the enzymes with the substrate because of their binding tendency to identical active sites. Therefore, those products act like inhibitors and displace the substrate from the active site of the enzymes and form an enzyme-inhibitor complex ultimately leading to loss of enzymes. A thermodynamic principle explains this inhibitory mechanism more accurately. Two equilibria, one between enzyme and inhibitors/products and the other between enzyme and substrate, exist in parallel and these two equilibria are not independent as the enzyme-substrate complex and enzyme-inhibitor complex equilibrate with the same free enzyme pool. Therefore, increasing enzyme-substrate concentration is the only way to eliminate the probability of enzyme-inhibitor complex formation. Increasing the substrate concentration from 25 g/L to 50 g/L offers more substrate for a particular enzyme concentration which in turn forms enzyme-substrate complex more frequently than enzyme-inhibitor complex. This supports the presence of competitive inhibition exerted by glucose. On the other hand, in noncompetitive inhibition, glucose would bind to the allosteric sites of the enzymes, thereby reducing its surface activity and inhibiting the enzyme non-competitively. Glucose has an equal binding affinity to both the free enzymes and the enzyme-substrate complex. In the present study, constants associated with competitive and noncompetitive inhibition are evaluated using equations (3) and (4) and presented in Table 5.

Table 5 Estimated parameters of inhibition kinetics.

Enzyme concentration (g/L)	Substrate concentration (g/L)	Competitive			Noncompetitive		
		k_m (g/L)	k_{cat} (sec^{-1})	K_i (g/L)	k_m (g/L)	k_{cat} (sec^{-1})	K_i (g/L)
1.28	25	2.288	0.142	1.594	0.057	.321	1.152

	50	2.274	.185	1.71	159.73	1.55	9.41
	125	2.227	.113	.658	-54.44	$.723\times10^{6}$	.088
6.66	25	2.206	0.027	1.673	1.34	-12.29	-0.005
	50	3.922	0.111	2.213	1.326×10^{6}	6.02×10^{3}	14.39
	125	.865	0.024	.786	11.94	-20.715	-0.006
11.23	25	3.652	0.032	2.248	1.407	-6.2	-0.012
	50	4.222	0.065	2.816	432.89	0.91	48.34
	125	1.08	0.019	.938	16.19	-12.57	-0.012
17.8	25	6.162	0.027	3.196	1.33	-4.37	-0.012
	50	9.766	0.058	6.322	70.65	0.13	45.77
	125	1.140	.014	.992	5.99	-9.84	-0.009

The value of inhibition constant increased gradually with escalated enzyme concentration for a particular substrate loading during competitive inhibition (refer Table 5), indicating reduced inhibition by the product formed. The same trend is also observed for a particular enzyme concentration with escalated substrate concentration from 25 g/L to 50 g/L. However, for a particular enzyme concentration, value of the inhibition constant decreased when the substrate loading was increased to 125 g/L. As discussed above, this is due to the film resistance created by the formation of thick slurry at such high substrate concentrations and nonproductive irreversible adsorption of enzymes on surfaces of substrate. Enzymatic hydrolysis with a loading of 50 g/L substrate, along with 17.8 g/L

enzyme concentration, is found optimum with an inhibition constant of 6.322 with minimum inhibition and maximum production of sugars. On the contrary, in case of noncompetitive inhibition, many of the kinetic constants appear with negative values which make this mode of inhibition unlikely for the current study. In early studies negative kinetic constants were also found for noncompetitive inhibition when pretreated cellulose was hydrolyzed with cellulase enzyme system [enzyme commission no.: *3.2.1.4*](Caminal, Lopez-Santin, & Sola, 1985). It can be inferred that the product inhibition of the system studied here follows a competitive mode of inhibition. The theoretical data set, evaluated using the competitive kinetic constants in equation (3), is compared with experimental data and represented in Fig.6 with a value of $r^2 \geq 0.91$ except for the system composed of 125 g/L substrate and 1.28 g/L enzyme ($r^2=0.89$).

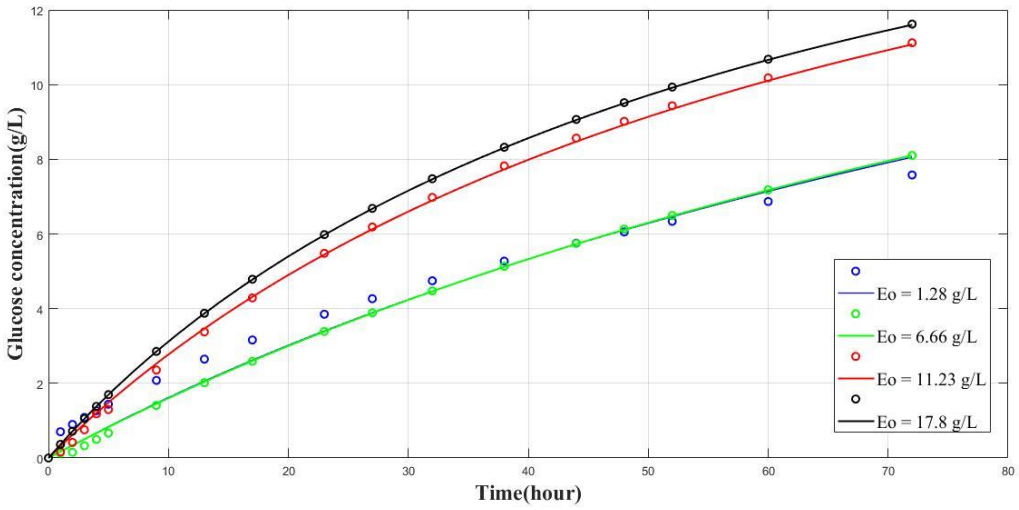

Figure 6(a)

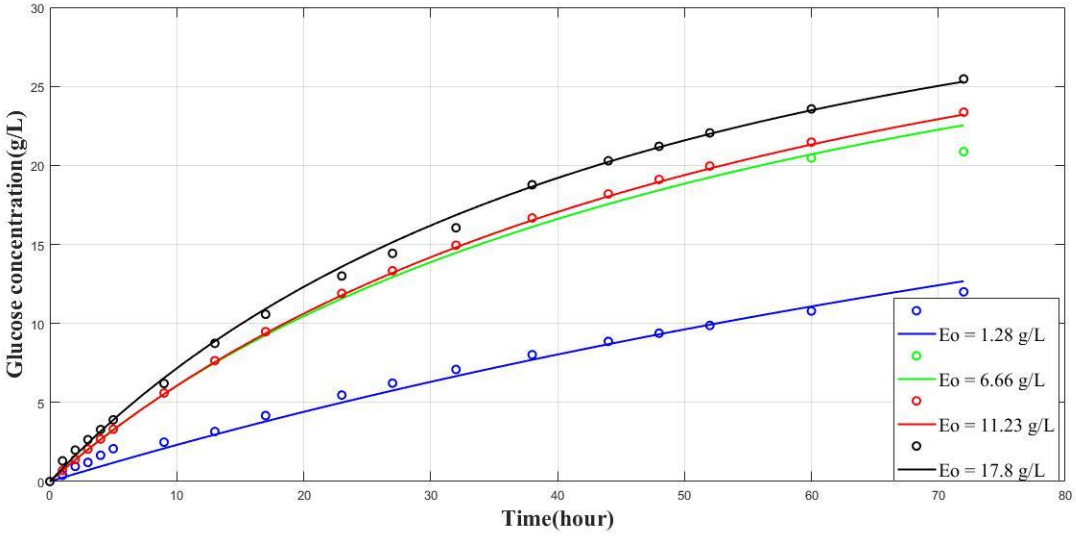

Figure 6(b)

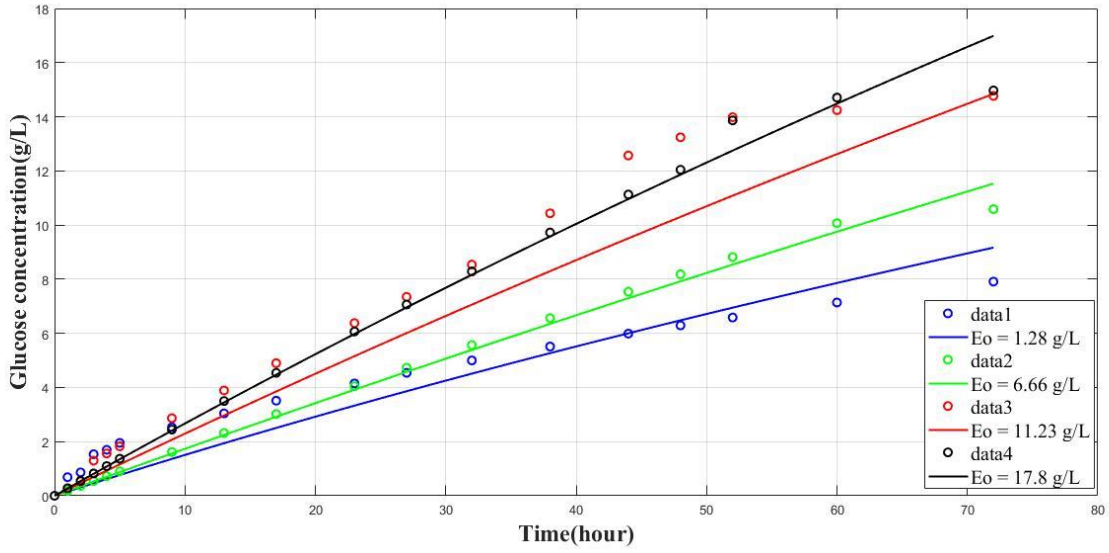

Figure 6(c)

Figure 6 Predicted inhibition model outputs (curves with solid lines) along with observed data (markers) for enzymatic hydrolysis of (a) 25g/L, (b) 50 g/L and (c) 125 g/L pretreated substrate with various enzyme concentrations.

3.6. Effect of each pretreatment step on enzymatic hydrolysis outcome

In order to understand the effect of each pretreatment step on enzymatic hydrolysis, substrate of a constant concentration (50 g/l) is withdrawn after each pretreatment process and hydrolyzed with four known enzyme concentrations (1.28, 6.66, 11.23 and 17.8 g/l) [See Figure 7 and Figure 8]. Additionally, recovery of glucan and xylan after hydrolysis of the autoclaved and probe sonicated biomass is assessed in order to understand the effect of each step of combined pretreatment on hydrolysis.

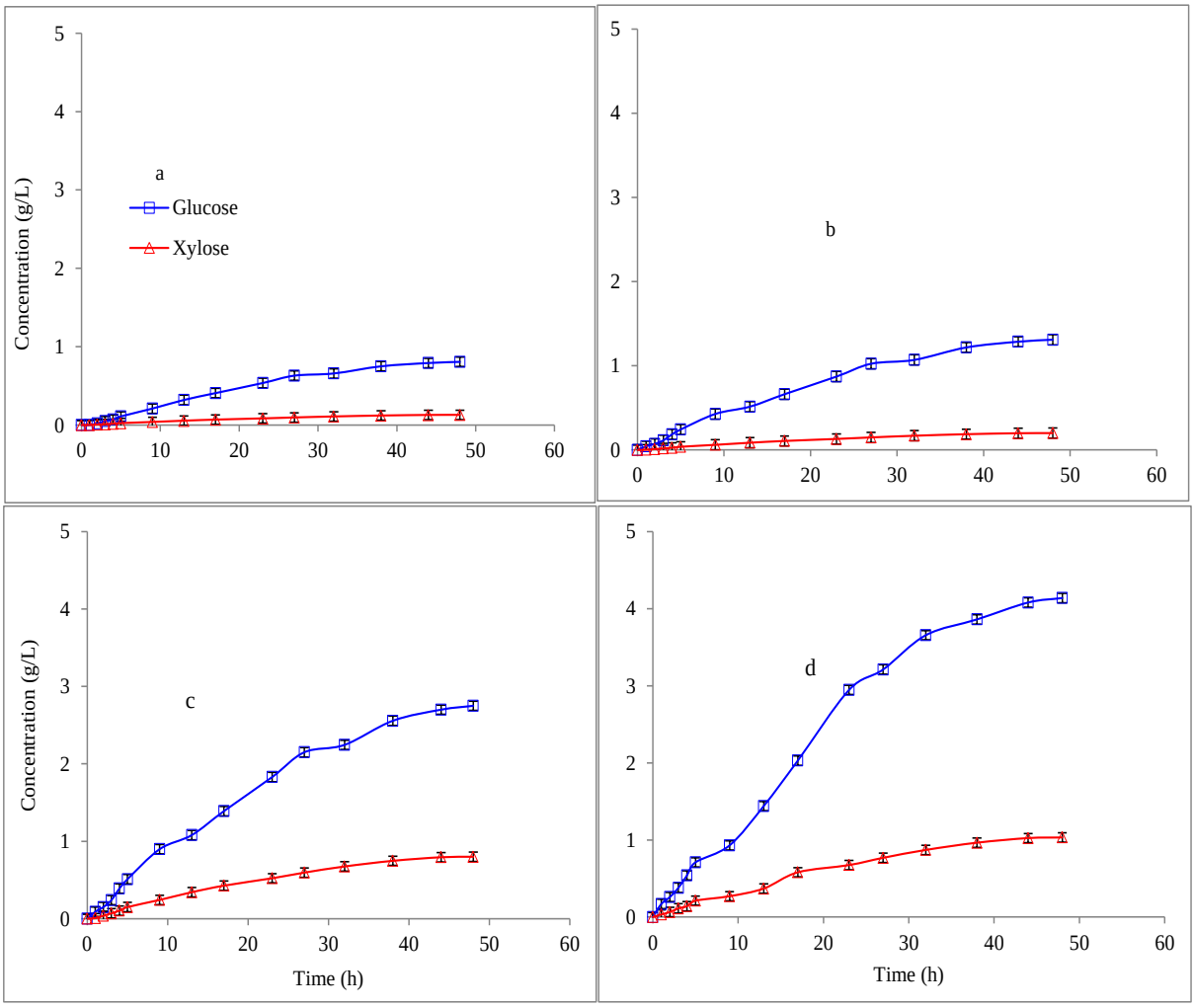

Figure 7 Enzymatic hydrolysis of autoclaved substrate (50 g/L) with different known enzyme concentrations [(a) 1.28 g/L, (b) 6.66 g/L, (c) 11.23 g/L, (d) 17.8 g/L].

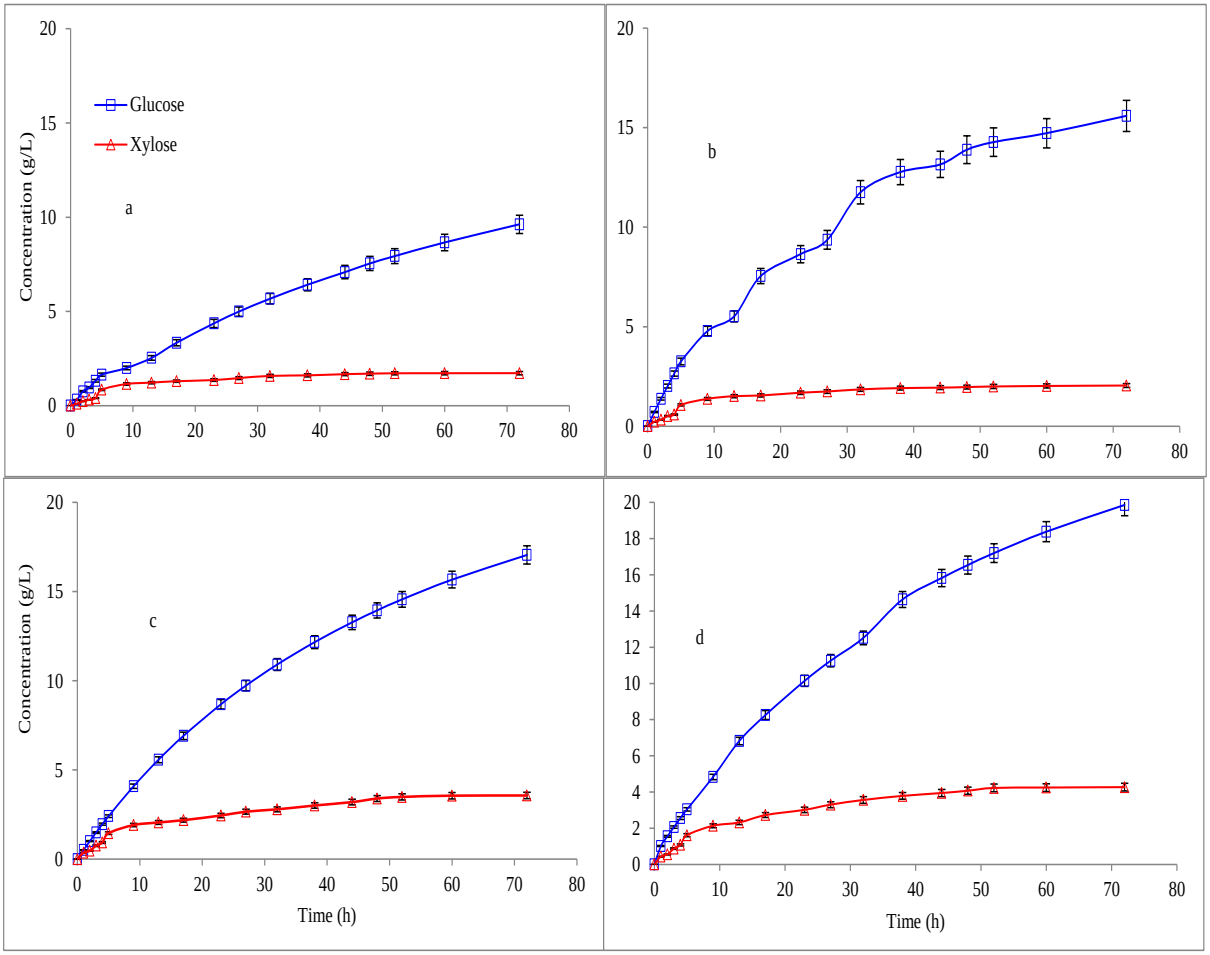

Figure 8 Enzymatic hydrolysis of probe sonicated substrate (50 g/L) with different known enzyme concentrations [(a) 1.28 g/L, (b) 6.66 g/L, (c) 11.23 g/L, (d) 17.8 g/L].

Table 6 Recovery of glucan and xylan (wt %) after hydrolysis using each step of combined pretreatment (CP) of the LB (substrate).

Pretreatment step	Substrate concentration (g/L)	Enzyme Concentration (g/L)	Carbohydrate conversion and yield			
			Glucan conversion (%)	Glucose Yield (%)	Xylan conversion (%)	Xylose Yield(%)

Autoclaved	50	1.28	3.06	2.754	1.44	1.2672
		6.66	4.97	4.473	2.23	1.9624
		11.23	10.50	9.45	8.90	7.832
		17.8	15.84	14.256	11.47	10.0936
Probe sonicated	50	1.28	34.09	30.681	19.01	16.7288
		6.66	55.24	49.716	23.11	20.3368
		11.23	60.42	54.378	40.29	35.4552
		17.8	70.38	63.342	48.3	42.504

It can be seen from the Figures (refer Figure 7 and Figure 8) that a minor amount of glucose and xylose are generated following hydrolysis of autoclaved substrate. Using lower concentration of enzymes like 1.28 g/L, only 3.06% glucan and 1.44% of xylan get converted. Additionally, elevated yield of carbohydrate is accomplished with augmented enzyme concentration with a corresponding yield of 14.256% glucose and 10.094% of xylose (*enzyme concentration*: 17.8g/L). After autoclaving, the substrate still contains considerable amount of lignin which is responsible for the irreversible and non-productive binding of supplied enzymes on lignin surface. On the other hand, autoclaving helps in the solubilization of lignin and hemicellulose side chains, keeping crystallinity of cellulose unaffected. As a result, enzymes cannot substantially de-polymerize lignocellulosic carbohydrates. On the contrary, better results are observed when probe sonicated substrate (50g/L) is hydrolyzed with same enzyme concentrations [(a) 1.28 g/L,

(b) 6.66 g/L, (c) 11.23 g/L, (d) 17.8 g/L]. The highest level of glucose and xylose yield are 63.342% and 42.504% respectively, following hydrolysis of probe sonicated substrate with 17.8 g/L enzyme concentration. Probe sonication helps in the removal of amorphous cellulosic materials along with considerable amount of lignin. Supplied enzymes can thus access crystalline cellulose. Therefore, following hydrolysis of probe sonicated material, an elevated concentration of glucose and xylose is observed.

4. Conclusion

By systematically comparing two different pretreatment methods (CP and AP), CP is found to be a better option in terms of preparation of biomass for subsequent enzymatic hydrolysis as it increases the accessible surface area of biomass for accommodating enzymes in the active sites as well as increases the crystallinity. Appropriate enzyme loading per unit substrate mass is found to be a crucial factor for optimal hydrolysis outcomes. Enzyme cocktails used in the present study are found to be inhibited competitively with produced glucose (*product inhibition*). Apart from enzyme and substrate loadings, the role of water is also found to be crucial for retaining the optimum activity of enzymes and for efficient hydrolysis of substrates. Lack of sufficient water in slurry (with large fraction of solids) hinders the free movement and mixing of enzymes with its substrates, eventually leading to inefficient hydrolysis. This condition even inhibits the enzymes at a relatively early stage of hydrolysis.

Acknowledgements

This work is a part of a collaborative research work under a joint Indo (DST)-Norway (RCN) project. The Indian side has been supported and funded by Department of Science and

Technology (DST), Government of India under Grant no: DST/INT/Nor/RCN/P-06/2015. The Norwegian side has been funded by the Research Council of Norway (RCN) under grant no. 246821/E20 (*EcoLodge*). The author Dr.J.C. Kuniyal heartily thanks to the Director, G.B. Pant National Institute of Himalayan Environment and Sustainable Development, Kosi-Katarmal-263643, Uttarakhand, India for providing necessary facilities in the Institute.

References

Agbor, V. B., Cicek, N., Sparling, R., Berlin, A., & Levin, D. B. (2011). Biomass pretreatment: fundamentals toward application. *Biotechnology advances, 29*(6), 675-685.

Alvarez-Vasco, C., & Zhang, X. (2013). Alkaline hydrogen peroxide pretreatment of softwood: hemicellulose degradation pathways. *Bioresource technology, 150*, 321-327.

Andrić, P., Meyer, A. S., Jensen, P. A., & Dam-Johansen, K. (2010). Reactor design for minimizing product inhibition during enzymatic lignocellulose hydrolysis: I. Significance and mechanism of cellobiose and glucose inhibition on cellulolytic enzymes. *Biotechnology advances, 28*(3), 308-324.

Arya, S., Kalia, R., & Arya, I. (2000). Induction of somatic embryogenesis in Pinus roxburghii Sarg. *Plant Cell Reports, 19*(8), 775-780.

Baksi, S., Saha, S., Birgen, C., Sarkar, U., Preisig, H. A., Markussen, S., . . . Wentzel, A. (2018). Valorization of Lignocellulosic Waste (Crotalaria juncea) Using Alkaline Peroxide Pretreatment under Different Process Conditions: An Optimization Study on Separation of Lignin, Cellulose, and Hemicellulose. *Journal of Natural Fibers*, 1-15.

552 Banerjee, G., Car, S., Scott-Craig, J. S., Hodge, D. B., & Walton, J. D. (2011). Alkaline
553 peroxide pretreatment of corn stover: effects of biomass, peroxide, and enzyme
554 loading and composition on yields of glucose and xylose. *Biotechnology for biofuels, 4*(1), 16.
555
556 Barr, C. J., Mertens, J. A., & Schall, C. A. (2012). Critical cellulase and hemicellulase
557 activities for hydrolysis of ionic liquid pretreated biomass. *Bioresource technology, 104*, 480-485.
558
559 Betts, W., Dart, R., Ball, A., & Pedlar, S. (1991). Biosynthesis and structure of
560 lignocellulose. In *Biodegradation* (pp. 139-155): Springer.
561 Bezerra, R. M., Dias, A. A., Fraga, I., & Pereira, A. N. (2006). Simulaaneous ethanol and
562 cellobiose inhibition of cellulose hydrolysis studied with integrated equations
563 assuming constant or variable substrate concentration. *Applied biochemistry and*
564 *biotechnology, 134*(1), 27-38.
565 Caminal, G., Lopez-Santin, J., & Sola, C. (1985). Kinetic modeling of the enzymatic
566 hydrolysis of pretreated cellulose. *Biotechnology and Bioengineering, 27*(9), 1282-
567 1290.
568 Chen, S., Ling, Z., Zhang, X., Kim, Y. S., & Xu, F. (2018). Towards a multi-scale
569 understanding of dilute hydrochloric acid and mild 1-ethyl-3-methylimidazolium
570 acetate pretreatment for improving enzymatic hydrolysis of poplar wood. *Industrial*
571 *Crops and Products, 114*, 123-131.
572 Chen, W.-H., Hsu, H.-C., Lu, K.-M., Lee, W.-J., & Lin, T.-C. (2011). Thermal pretreatment
573 of wood (Lauan) block by torrefaction and its influence on the properties of the
574 biomass. *Energy, 36*(5), 3012-3021.

575 Corazza, F., Calsavara, L., Moraes, F., Zanin, G., & Neitzel, I. (2005). Determination of
576 inhibition in the enzymatic hydrolysis of cellobiose using hybrid neural modeling.
577 *Brazilian Journal of Chemical Engineering, 22*(1), 19-29.
578 Fang, J., Sun, R., & Tomkinson, J. (2000). Isolation and characterization of hemicelluloses
579 and cellulose from rye straw by alkaline peroxide extraction. *Cellulose, 7*(1), 87-107.
580 Fenila, F., & Shastri, Y. (2016). Optimal control of enzymatic hydrolysis of lignocellulosic
581 biomass. *Resource-Efficient Technologies, 2*, S96-S104.
582 Geng, Z., Sun, R., Sun, X., & Lu, Q. (2003). Comparative study of hemicelluloses released
583 during two-stage treatments with acidic organosolv and alkaline peroxide from
584 Caligonum monogoliacum and Tamarix spp. *Polymer degradation and stability,*
585 *80*(2), 315-325.
586 Hu, F., & Ragauskas, A. (2012). Pretreatment and lignocellulosic chemistry. *Bioenergy*
587 *Research, 5*(4), 1043-1066.
588 Lai, C., Tu, M., Shi, Z., Zheng, K., Olmos, L. G., & Yu, S. J. B. t. (2014). Contrasting effects
589 of hardwood and softwood organosolv lignins on enzymatic hydrolysis of
590 lignocellulose. *163*, 320-327.
591 Lavoine, N., Desloges, I., Dufresne, A., & Bras, J. (2012). Microfibrillated cellulose–Its
592 barrier properties and applications in cellulosic materials: A review. *Carbohydrate*
593 *polymers, 90*(2), 735-764.
594 Lee, Y. H., & Fan, L. (1983). Kinetic studies of enzymatic hydrolysis of insoluble
595 cellulose:(II). Analysis of extended hydrolysis times. *Biotechnology and*
596 *Bioengineering, 25*(4), 939-966.
597 Li, M., Tu, M., Cao, D., Bass, P., Adhikari, S. J. J. o. a., & chemistry, f. (2013). Distinct roles
598 of residual xylan and lignin in limiting enzymatic hydrolysis of organosolv pretreated
599 loblolly pine and sweetgum. *61*(3), 646-654.

600 Lin, L., Yan, R., Liu, Y., & Jiang, W. J. B. T. (2010). In-depth investigation of enzymatic
601 hydrolysis of biomass wastes based on three major components: cellulose,
602 hemicellulose and lignin. *101*(21), 8217-8223.
603 Luo, C., Brink, D. L., & Blanch, H. W. (2002). Identification of potential fermentation
604 inhibitors in conversion of hybrid poplar hydrolyzate to ethanol. *Biomass and*
605 *bioenergy, 22*(2), 125-138.
606 Miller, G. L. (1959). Use of dinitrosalicylic acid reagent for determination of reducing sugar.
607 *Analytical chemistry, 31*(3), 426-428.
608 O'Dwyer, J. P., Zhu, L., Granda, C. B., & Holtzapple, M. T. (2007). Enzymatic hydrolysis of
609 lime-pretreated corn stover and investigation of the HCH-1 model: inhibition pattern,
610 degree of inhibition, validity of simplified HCH-1 model. *Bioresource technology,*
611 *98*(16), 2969-2977.
612 Qing, Q., & Wyman, C. E. (2011). Supplementation with xylanase and β-xylosidase to
613 reduce xylo-oligomer and xylan inhibition of enzymatic hydrolysis of cellulose and
614 pretreated corn stover. *Biotechnology for biofuels, 4*(1), 18.
615 Sargent, C. S. (1896). *The silva of North America: a description of the trees which grow*
616 *naturally in North America exclusive of Mexico* (Vol. 9): Houghton, Mifflin.
617 Sluiter, A., Hames, B., Ruiz, R., Scarlata, C., Sluiter, J., Templeton, D., & Crocker, D.
618 (2008). Determination of structural carbohydrates and lignin in biomass. *Laboratory*
619 *analytical procedure, 1617*, 1-16.
620 Standard, T. (2002). Acid-insoluble lignin in wood and pulp. *T222 om-02*.
621 Sternberg, D., Vuayakumar, P., & Reese, E. (1977). β-Glucosidase: microbial production and
622 effect on enzymatic hydrolysis of cellulose. *Canadian Journal of Microbiology,*
623 *23*(2), 139-147.

624 Subhedar, P. B., & Gogate, P. R. (2014). Alkaline and ultrasound assisted alkaline
625 pretreatment for intensification of delignification process from sustainable raw-
626 material. *Ultrasonics sonochemistry, 21*(1), 216-225.
627 Sun, J., Mao, F., Sun, X., & Sun, R. (2005). Comparative study of hemicelluloses isolated
628 with alkaline peroxide from lignocellulosic materials. *Journal of wood chemistry and*
629 *technology, 24*(3), 239-262.
630 Sun, Y., & Cheng, J. (2002). Hydrolysis of lignocellulosic materials for ethanol production: a
631 review. *Bioresource Technology, 83*(1), 1-11.
632 Sun, Y., & Cheng, J. J. (2005). Dilute acid pretreatment of rye straw and bermudagrass for
633 ethanol production. *Bioresource technology, 96*(14), 1599-1606.
634 Tappi, T. (2002). 222 om-02: Acid-insoluble lignin in wood and pulp. *2002–2003 TAPPI*
635 *Test Methods*.
636 Van Wychen, S., & Laurens, L. (2017). Total Carbohydrate Content Determination of
637 Microalgal Biomass by Acid Hydrolysis Followed by Spectrophotometry or Liquid
638 Chromatography.
639 Wang, Z., Keshwani, D. R., Redding, A. P., & Cheng, J. J. (2010). Sodium hydroxide
640 pretreatment and enzymatic hydrolysis of coastal Bermuda grass. *Bioresource*
641 *technology, 101*(10), 3583-3585.
642 Wigell, A., Brelid, H., & Theliander, H. (2007). Degradation/dissolution of softwood
643 hemicellulose during alkaline cooking at different temperatures and alkali
644 concentrations. *Nordic Pulp & Paper Research Journal, 22*(4), 488-494.
645 Wu, J., Yu, D., Chan, C. M., Kim, J., & Mai, Y. W. (2000). Effect of fiber pretreatment
646 condition on the interfacial strength and mechanical properties of wood fiber/PP
647 composites. *Journal of applied polymer science, 76*(7), 1000-1010.

Wyman, C. E., Decker, S. R., Himmel, M. E., Brady, J. W., Skopec, C. E., & Viikari, L. (2005). Hydrolysis of cellulose and hemicellulose. *Polysaccharides: Structural diversity and functional versatility, 1*, 1023-1062.

Xiao, Z., Zhang, X., Gregg, D. J., & Saddler, J. N. (2004). *Effects of sugar inhibition on cellulases and β-glucosidase during enzymatic hydrolysis of softwood substrates.* Paper presented at the Proceedings of the Twenty-Fifth Symposium on Biotechnology for Fuels and Chemicals Held May 4–7, 2003, in Breckenridge, CO.

Xu, J., Cheng, J. J., Sharma-Shivappa, R. R., & Burns, J. C. (2010). Sodium hydroxide pretreatment of switchgrass for ethanol production. *Energy & Fuels, 24*(3), 2113-2119.

Yoon, H., Wu, Z., & Lee, Y. (1995). Ammonia-recycled percolation process for pretreatment of biomass feedstock. *Applied biochemistry and biotechnology, 51*(1), 5-19.

Zhang, J., Feng, L., Wang, D., Zhang, R., Liu, G., & Cheng, G. (2014). Thermogravimetric analysis of lignocellulosic biomass with ionic liquid pretreatment. *Bioresource technology, 153*, 379-382.

Zhao, Y., Wu, B., Yan, B., & Gao, P. (2004). Mechanism of cellobiose inhibition in cellulose hydrolysis by cellobiohydrolase. *Science in China Series C: Life Sciences, 47*(1), 18-24.

Zhu, J. Y., Pan, X., & Zalesny, R. S. (2010). Pretreatment of woody biomass for biofuel production: energy efficiency, technologies, and recalcitrance. *Applied microbiology and biotechnology, 87*(3), 847-857.